



CERN-EP-2020-224
 LHCb-PAPER-2020-038
 January 15, 2021

First observation of the decay $B_s^0 \rightarrow K^- \mu^+ \nu_\mu$ and a measurement of $|V_{ub}|/|V_{cb}|$

LHCb collaboration[†]

Abstract

The first observation of the suppressed semileptonic $B_s^0 \rightarrow K^- \mu^+ \nu_\mu$ decay is reported. Using a data sample recorded in pp collisions in 2012 with the LHCb detector, corresponding to an integrated luminosity of 2 fb^{-1} , the branching fraction $\mathcal{B}(B_s^0 \rightarrow K^- \mu^+ \nu_\mu)$ is measured to be $(1.06 \pm 0.05\text{ (stat)} \pm 0.08\text{ (syst)}) \times 10^{-4}$, where the first uncertainty is statistical and the second one represents the combined systematic uncertainties. The decay $B_s^0 \rightarrow D_s^- \mu^+ \nu_\mu$, where D_s^- is reconstructed in the final state $K^+ K^- \pi^-$, is used as a normalization channel to minimize the experimental systematic uncertainty. Theoretical calculations on the form factors of the $B_s^0 \rightarrow K^-$ and $B_s^0 \rightarrow D_s^-$ transitions are employed to determine the ratio of the CKM matrix elements $|V_{ub}|/|V_{cb}|$ at low and high $B_s^0 \rightarrow K^-$ momentum transfer.

Published in Phys. Rev. Lett.

© 2021 CERN for the benefit of the LHCb collaboration. CC BY 4.0 licence.

[†]Authors are listed at the end of this paper.

The coupling of the electroweak interaction between up- and down-type quarks is modulated by the Cabibbo-Kobayashi-Maskawa (CKM) matrix [1, 2]. Hadrons containing a b quark can decay weakly via a virtual W boson to semileptonic final states through the tree-level transitions $b \rightarrow c(W^* \rightarrow \ell\nu)$ and $b \rightarrow u(W^* \rightarrow \ell\nu)$, where $\ell\nu$ denotes a charged lepton and a neutrino. These transitions involve the CKM matrix elements V_{cb} and V_{ub} , respectively, which obey the observed hierarchy $|V_{ub}|/|V_{cb}| \sim 0.1$, resulting in the transitions $b \rightarrow cl\nu$ being favored over $b \rightarrow ul\nu$. Semileptonic b -hadron decays are an excellent ground for measuring $|V_{cb}|$ and $|V_{ub}|$ since the factorization of the hadronic and leptonic parts of the amplitudes eases theoretical calculations [3, 4]. Improving the precision on the measurements of the CKM elements can be exploited to probe possible deviations from the Standard Model of particle physics [5]. Existing $|V_{ub}|$ and $|V_{cb}|$ measurements show a discrepancy between those performed with exclusive decays, where all the visible particles are reconstructed, and inclusive decays where only the lepton is reconstructed [6]. The world average of the exclusive $|V_{ub}|$ results is dominated by $B^0 \rightarrow \pi^- \ell^+ \nu_\ell$ measurements. The LHCb measurement using the baryonic decays $\Lambda_b^0 \rightarrow p \mu^- \bar{\nu}_\mu$ and $\Lambda_b^0 \rightarrow \Lambda_c^+ \mu^- \bar{\nu}_\mu$ [7] gives the ratio $|V_{ub}|/|V_{cb}| = 0.079 \pm 0.006$, as updated in Ref. [6]. Besides the inclusive versus exclusive puzzle, measurements of $|V_{ub}|/|V_{cb}|$ are important to constrain the CKM unitarity triangle [8, 9].

This Letter reports the first observation of the decay $B_s^0 \rightarrow K^- \mu^+ \nu_\mu$, the measurement of its branching fraction and of the ratio $|V_{ub}|/|V_{cb}|$ with $B_s^0 \rightarrow D_s^- \mu^+ \nu_\mu$ as a normalization channel.¹ The measurement of the branching fraction is performed in two regions of the $B_s^0 \rightarrow K^-$ momentum transfer or invariant mass squared of the muon and the neutrino, q^2 , as well as integrated over the full q^2 range. The ratio $|V_{ub}|/|V_{cb}|$ is derived in the two q^2 regions using calculations of the form factors of the $B_s^0 \rightarrow K^-$ and $B_s^0 \rightarrow D_s^-$ transitions based on both light cone sum rule (LCSR) [10, 11] and lattice QCD (LQCD) [12] methods. The data sample consists of pp collisions recorded by the LHCb detector in 2012 at a center-of-mass energy of 8 TeV corresponding to 2 fb^{-1} of integrated luminosity. The LHCb detector is a single-arm forward spectrometer covering the pseudorapidity range $2 < \eta < 5$, described in detail in Refs. [13, 14]. The trigger [15] consists of a hardware stage, based on information from the calorimeter and muon systems, followed by a software stage, which reconstructs charged particles. Simulation, produced with software packages described in Refs. [16–18], is used to model the effects of the detector acceptance and the imposed selection requirements.

In this analysis candidates for $B_s^0 \rightarrow K^- \mu^+ \nu_\mu$ and $B_s^0 \rightarrow D_s^- \mu^+ \nu_\mu$ decays are formed by combining a muon with a kaon or a D_s^- candidate reconstructed through the decay $D_s^- \rightarrow K^+ K^- \pi^-$. The trigger and initial selection requirements are chosen to be similar between these two modes. Events are retained by the hardware trigger due to the presence of a high- p_T muon, where p_T is the momentum component transverse to the beam. The software trigger [19] selects partially reconstructed B decays by combining a track or a D_s^- candidate with a well identified muon candidate. The initial selection includes requirements on the track kinematics and quality, particle identification, as well as on the B_s^0 candidate kinematics and decay topology. The obtained samples for each of the decays include background contributions dominated by b -hadron decays with additional tracks or neutral particles in the final state. For the $K^- \mu^+$ combinations, the main background originates from $H_b \rightarrow \mu^+ H_c (\rightarrow K^- X) X'$, where $H_{b,c}$ represents a hadron containing a b

¹Throughout the paper, charge conjugate decays are implied.

or a c quark and $X^{(\prime)}$ denotes unreconstructed particles. Decays to excited K^* resonances, $B_s^0 \rightarrow K^{*-}(\rightarrow K^-\pi^0)\mu^+\nu_\mu$, and charmonium modes $B \rightarrow [c\bar{c}](\rightarrow \mu^+\mu^-)K^-X$, where $[c\bar{c}] = J/\psi, \psi(2S)$, are secondary background contributions. Other sources arise from b -hadron decays where a track is misidentified as a kaon or a muon, and random combinations of a muon and a kaon. In the $D_s^-\mu^+$ combinations, the main (and irreducible) source of background arises from $B_s^0 \rightarrow D_s^{*-}(\rightarrow D_s^-\gamma)\mu^+\nu_\mu$ decays. Additional contributions include decays to higher excitations of the D_s^- meson, $B_s^0 \rightarrow D_s^{**-}(\rightarrow D_s^-X)\mu^+\nu_\mu$, double-charm decays of the type $B_{u,d,s} \rightarrow D_sDX$ and semitauonic $B_s^0 \rightarrow D_s^-\tau^+\nu_\tau$ decays.

To suppress background, the $K^-\mu^+$ and $D_s^-\mu^+$ candidates are required to be isolated from other tracks in the event. A multivariate algorithm (MVA) is trained to determine if a given track originates from the candidate, or from the rest of the event (ROE). A threshold on the value of the MVA output is applied to the ROE track that appears to be the closest to the signal. For $K^-\mu^+$ candidates, two boosted decision tree (BDT) classifiers [20, 21] are used sequentially to further reduce the remaining background. A *charged* BDT classifier is trained against a mixture of the main background components using, in addition to the isolation MVA output, invariant masses formed by the least isolated ROE track with respect to each of the muon or the kaon, and variables related to the B_s^0 , K^- and μ^+ kinematics. The background passing the *charged* BDT requirement comprises decays without an additional track, mainly of the type $H_b \rightarrow \mu^+H_c(\rightarrow K^-P)$, where P is either a long-lived or a neutral particle. A second BDT classifier, denoted *neutral* BDT, involves kinematic variables of the K^- and B_s^0 candidates, the B_s^0 vertex position and quality, the invariant mass formed by the signal kaon and any π^0 meson in its vicinity; it also exploits the asymmetry between the kaon momentum and an average momentum direction formed by neutral particles in the vicinity of the kaon. The shapes of the BDT outputs are calibrated with the decay $B^- \rightarrow J/\psi(\rightarrow \mu^+\mu^-)K^-$, which is reconstructed both as a $K^-\mu^+$ candidate and fully reconstructed where the least isolated track near the $K^-\mu^+$ pair is identified as μ^- . Kinematic weighting accounts for data-simulation discrepancies for the training of the classifiers.

The B_s^0 mass is represented by the corrected mass [22], defined as

$$m_{\text{corr}} = \sqrt{m_{Y\mu}^2 + p_\perp^2/c^2} + p_\perp/c, \quad (1)$$

where $m_{Y\mu}$ is the invariant mass of the $Y\mu$ pair, with $Y = K^-$ or D_s^- , and p_\perp is the momentum of this pair transverse to the B_s^0 flight direction. The flight direction is defined as the vector between the positions of the primary pp collision vertex and the B_s^0 decay vertex. In order to improve the separation between the $B_s^0 \rightarrow K^-\mu^+\nu_\mu$ signal and background, the uncertainty on m_{corr} is required to be $\sigma(m_{\text{corr}}) < 100 \text{ MeV}/c^2$. The shape of $\sigma(m_{\text{corr}})$ is calibrated following a similar procedure as for the BDT classifiers. To derive q^2 , the neutrino momentum is estimated using the B_s^0 flight direction and the known B_s^0 mass. A two-fold ambiguity resulting from this estimate is resolved by choosing the solution that is most consistent with the B_s^0 momentum predicted by a linear regression method [23]. The fit to the m_{corr} distribution, used for the extraction of the $B_s^0 \rightarrow K^-\mu^+\nu_\mu$ signal, is performed in two q^2 regions, respectively above and below $7 \text{ GeV}^2/c^4$ (“high” and “low”), which are chosen to contain approximately the same expected signal yields.

For the $B_s^0 \rightarrow D_s^-\mu^+\nu_\mu$ decay, a fit to the invariant mass of the $D_s^- \rightarrow K^+K^-\pi^-$ candidates is performed in 40 intervals of m_{corr} from 3000 to $6500 \text{ MeV}/c^2$. This provides the D_s yield as a function of m_{corr} and thus subtracts the background originating from

combinations of random kaon and pion tracks. The obtained m_{corr} distribution is fit to extract the $B_s^0 \rightarrow D_s^- \mu^+ \nu_\mu$ signal yield. For the $B_s^0 \rightarrow K^- \mu^+ \nu_\mu$ decay, the combinatorial background is largely reduced by applying a topological criterion: the opening angle between the directions of the K^- and μ^+ candidates in the plane transverse to the pp collision axis is required to be less than 90 degrees. The efficiency of this requirement on the signal is 93%, while it removes approximately 90% of the combinatorial background.

The efficiencies of the signal and normalization channels are derived from simulation and take into account the effects of the triggers, reconstruction, selection, particle identification, isolation procedure, MVA requirements and detector acceptance. Data-driven corrections are applied to account for any mismodelling related to the kinematics, number of tracks in the event and particle identification variables. The efficiency ratio between the signal and normalization decays is $\epsilon_K/\epsilon_{D_s} = 1.109 \pm 0.018$, 0.553 ± 0.009 and 0.733 ± 0.009 for $q^2 < 7 \text{ GeV}^2/c^4$, $q^2 > 7 \text{ GeV}^2/c^4$ and the full q^2 range, respectively. The uncertainties reflect the limited size of the simulated samples.

The fit template for the m_{corr} distribution of the $B_s^0 \rightarrow K^- \mu^+ \nu_\mu$ signal is obtained from simulation, while the shapes for the background components are derived from either simulation or control samples. The statistical uncertainties originating from the finite samples used to obtain the templates are accounted for in the fits [24]. The main background $H_b \rightarrow H_c(\rightarrow K^- X) \mu^+ X'$, whose yield is free in the fit, is obtained with a simulated inclusive sample. The $B_s^0 \rightarrow K^{*-}(\rightarrow K^- \pi^0) \mu^+ \nu_\mu$ background is modelled by simulating a mixture of three resonances ($K^{*-}(892)$, $K_0^{*-}(1430)$ and $K_2^{*-}(1430)$) with a substantial branching fraction to the $K^- \pi^0$ final state. Though the overall yield is free, the mixture is fixed to certain proportions which are varied up to a factor of 2.5 for systematic studies, according to available measurements of the decays $B^- \rightarrow K^{*-} \mu^+ \mu^-$ and $B^- \rightarrow K^{*-} \eta/\phi$ [25]. The impact of a possible $B_s^0 \rightarrow K^- \pi^0 \mu^+ \nu_\mu$ nonresonant decay has also been considered and found to be absorbed by the resonant mixture. The charmonium background is dominated by $B^- \rightarrow J/\psi(\rightarrow \mu^+ \mu^-) K^- X$ decays, with the fraction of the $B^- \rightarrow J/\psi(\rightarrow \mu^+ \mu^-) K^-$ channel exceeding 75%. Its shape is determined with simulated $B^- \rightarrow J/\psi(\rightarrow \mu^+ \mu^-) K^- X$ events while its yield is derived from the yield of the $B^- \rightarrow J/\psi(\rightarrow \mu^+ \mu^-) K^-$ signal peak in data. To recover that peak from $K^- \mu^+$ combinations, the missing momentum of the μ^- is calculated from the B^- flight direction and the known J/ψ mass. The background originating from the misidentification (MisID) of a pion, proton or muon as a kaon; or a kaon, proton or pion as a muon is modelled using data samples of $h\mu^+$ ($K^- h$) candidates with an identical selection as for the main sample but where h is a charged track which fails the kaon (muon) identification criteria. These control samples are thus enriched in misidentified tracks of the different species. The different contributions to the kaon and muon MisID are unfolded using control samples of kinematically identified hadrons and muons [26]. These samples are used to derive the probabilities that a particle belonging to a given species and with particular kinematic properties would pass the kaon or muon criteria. With this method both the m_{corr} shape and the yield of the MisID are constrained. The combinatorial background is modelled with a separate data sample where a kaon and a muon from different events are combined. The obtained pseudocandidates undergo the same selection as the signal candidates and are corrected to reproduce the kinematic properties of the standard candidates.

The fit to the normalization channel $B_s^0 \rightarrow D_s^- \mu^+ \nu_\mu$ employs shapes obtained from simulation. The $B_s^0 \rightarrow D_s^- \mu^+ \nu_\mu$ decay is modelled with the recent form factor predictions of Ref. [27]. The main background originates from B_s^0 semimuonic decays to excitations

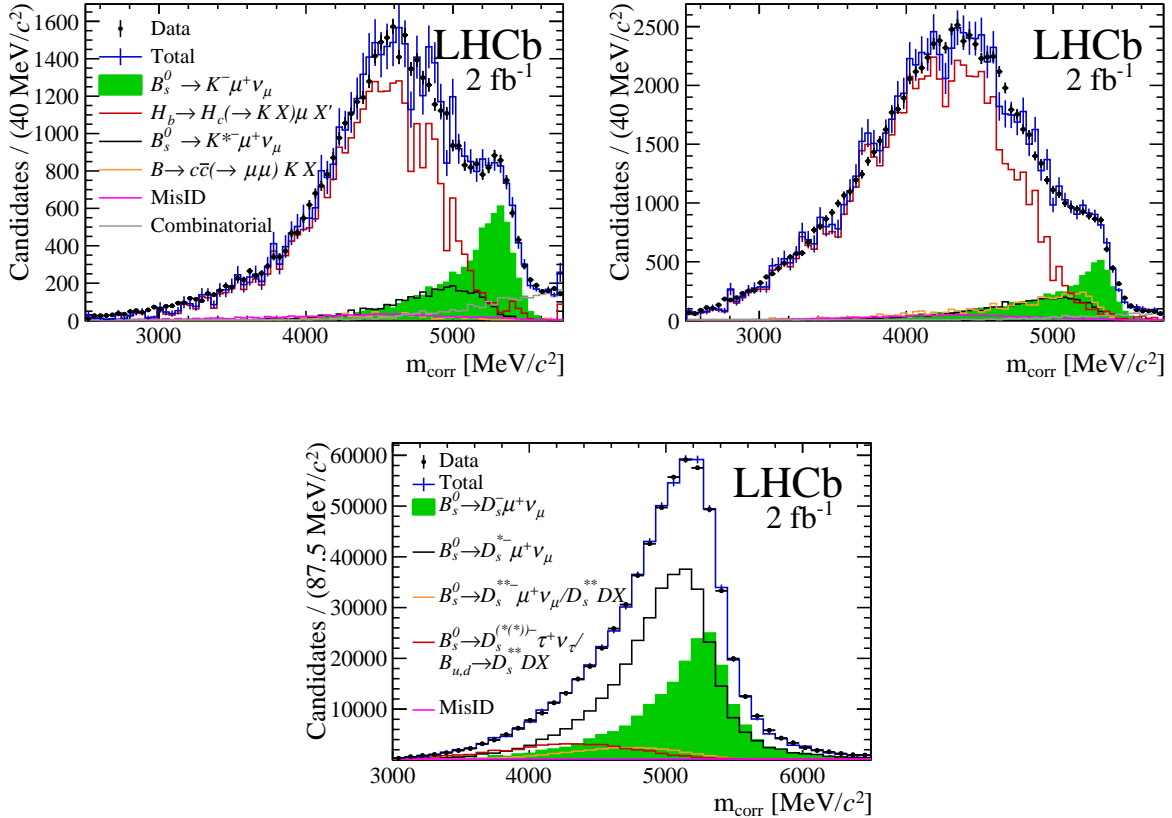


Figure 1: Distribution of m_{corr} for (top) the signal $B_s^0 \rightarrow K^- \mu^+ \nu_\mu$, with (left) $q^2 < 7 \text{ GeV}^2/c^4$ and (right) $q^2 > 7 \text{ GeV}^2/c^4$, and (bottom) the normalization $B_s^0 \rightarrow D_s^- \mu^+ \nu_\mu$ channel. The points represent data, while the resulting fit components are shown as histograms.

of the D_s^- meson, with the dominant $D_s^{*-} \rightarrow D_s^- \gamma$ decay represented by a specific shape, and higher excitations $D_s^{**-} = [D_{s0}^{*-}(2317), D_{s1}^{*-}(2460), D_{s1}^{*-}(2536)] \rightarrow D_s^- X$ modelled by a combined shape. Other sources of background are the decays of the form $B \rightarrow D_s^- DX$ and the semitauonic decay $B_s^0 \rightarrow D_s^- \tau^+(\rightarrow \mu^+ \nu_\mu \bar{\nu}_\tau) \nu_\tau$. Due to similarity of their shapes, the $B_s^0 \rightarrow D_s^{**-} \mu^+ \nu_\mu$ channels are grouped with $B_s \rightarrow D_s^- DX$ decays, while $B_s^0 \rightarrow D_s^- \tau^+(\rightarrow \mu^+ \nu_\mu \bar{\nu}_\tau) \nu_\tau$ is combined with $B_{u,d} \rightarrow D_s^- DX$ decays.

The corrected mass distributions of the signal and normalization candidates are shown in Fig. 1, with the binned maximum-likelihood fit projections overlaid. The $B_s^0 \rightarrow K^- \mu^+ \nu_\mu$ yields for $q^2 < 7 \text{ GeV}^2/c^4$ and $q^2 > 7 \text{ GeV}^2/c^4$ regions are found to be $N_K = 6922 \pm 285$ and 6399 ± 370 , respectively, while the $B_s^0 \rightarrow D_s^- \mu^+ \nu_\mu$ yield is $N_{D_s} = 201450 \pm 5200$. The uncertainties include both the effect of the limited data set and the finite size of the samples used to derive the fit templates. Unfolding the two effects in quadrature shows that they have similar sizes.

This is the first observation of the decay $B_s^0 \rightarrow K^- \mu^+ \nu_\mu$. The ratio of branching fractions is inferred as

$$R_{\text{BF}} \equiv \frac{\mathcal{B}(B_s^0 \rightarrow K^- \mu^+ \nu_\mu)}{\mathcal{B}(B_s^0 \rightarrow D_s^- \mu^+ \nu_\mu)} = \frac{N_K}{N_{D_s}} \frac{\epsilon_{D_s}}{\epsilon_K} \times \mathcal{B}(D_s^- \rightarrow K^+ K^- \pi^-), \quad (2)$$

Table 1: Relative systematic uncertainties on the ratio $\mathcal{B}(B_s^0 \rightarrow K^- \mu^+ \nu_\mu)/\mathcal{B}(B_s^0 \rightarrow D_s^- \mu^+ \nu_\mu)$, in percent.

Uncertainty	All q^2	low q^2	high q^2
Tracking	2.0	2.0	2.0
Trigger	1.4	1.2	1.6
Particle identification	1.0	1.0	1.0
$\sigma(m_{\text{corr}})$	0.5	0.5	0.5
Isolation	0.2	0.2	0.2
Charged BDT	0.6	0.6	0.6
Neutral BDT	1.1	1.1	1.1
q^2 migration	—	2.0	2.0
Efficiency	1.2	1.6	1.6
Fit template	+2.3 -2.9	+1.8 -2.4	+3.0 -3.4
Total	+4.0 -4.3	+4.3 -4.5	+5.0 -5.3

with $\mathcal{B}(D_s^- \rightarrow K^+ K^- \pi^-) = (5.39 \pm 0.15)\%$ [25] and gives

$$\begin{aligned} R_{\text{BF}}(\text{low}) &= (1.66 \pm 0.08 \text{ (stat)} \pm 0.07 \text{ (syst)} \pm 0.05 \text{ } (D_s)) \times 10^{-3}, \\ R_{\text{BF}}(\text{high}) &= (3.25 \pm 0.21 \text{ (stat)}^{+0.16}_{-0.17} \text{ (syst)} \pm 0.09 \text{ } (D_s)) \times 10^{-3}, \\ R_{\text{BF}}(\text{all}) &= (4.89 \pm 0.21 \text{ (stat)}^{+0.20}_{-0.21} \text{ (syst)} \pm 0.14 \text{ } (D_s)) \times 10^{-3}, \end{aligned}$$

where the uncertainties are statistical, systematic and due to the $D_s^- \rightarrow K^+ K^- \pi^-$ branching fraction. Table 1 summarizes the systematic uncertainties. It includes uncertainties on the calibration and correction of the track reconstruction, trigger, particle identification, selection variables, migration of events between q^2 regions, efficiencies and the fit template distributions. The largest systematic uncertainty originates from the fit templates and is evaluated by varying the shape of the fit components according to alternative models and also by modifying within its uncertainty the mixture of exclusive decays representing some of the background contributions. In particular, the signal shape is varied using various form factor models [28–31]. A similar procedure is applied to the normalization channel. The tracking uncertainty comprises the limited precision on tracking efficiency corrections obtained from control samples in data, and the uncertainty on modelling the hadronic interactions with the detector material. The uncertainty on the q^2 migration is related to the limited accuracy of the evaluation of the cross-feed between low and high q^2 regions in simulation.

To determine the branching fraction $\mathcal{B}(B_s^0 \rightarrow K^- \mu^+ \nu_\mu)$ and the ratio $|V_{ub}|/|V_{cb}|$, the predicted integrals of the form factors $\text{FF}_Y = |V_{xb}|^{-2} \int \frac{d\Gamma(B_s^0 \rightarrow Y \mu^+ \nu_\mu)}{dq^2} dq^2$ ($Y = K^-, D_s^-$; $x = u, c$) are required. The absolute branching fraction is calculated as $\mathcal{B}(B_s^0 \rightarrow K^- \mu^+ \nu_\mu) = \tau_{B_s} \times |V_{cb}|^2 \times \text{FF}_{D_s} \times R_{\text{BF}}$. The inputs are the exclusive value of $|V_{cb}| = (39.5 \pm 0.9) \times 10^{-3}$ [25], the B_s^0 meson lifetime $\tau_{B_s} = 1.515 \pm 0.004 \text{ ps}$ [25] and the form factor integral $\text{FF}_{D_s} = 9.15 \pm 0.37 \text{ ps}^{-1}$ based on a recent LQCD computation [27]. This leads to

$$\mathcal{B}(B_s^0 \rightarrow K^- \mu^+ \nu_\mu) = (1.06 \pm 0.05 \text{ (stat)} \pm 0.04 \text{ (syst)} \pm 0.06 \text{ (ext)} \pm 0.04 \text{ (FF)}) \times 10^{-4},$$

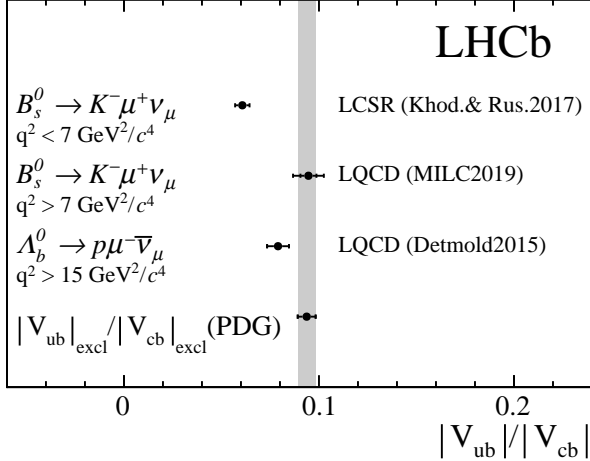


Figure 2: Measurements of $|V_{ub}|/|V_{cb}|$ in this Letter and in Ref. [7], and ratio inferred from the PDG [25] averages of exclusive $|V_{ub}|$ and $|V_{cb}|$ measurements, where the $\Lambda_b^0 \rightarrow p \mu^- \bar{\nu}_\mu$ result is not included. The form factor calculation used in each case is mentioned [30–32].

where the uncertainties are statistical, systematic, from the external inputs (D_s^- branching fraction, B_s^0 lifetime and $|V_{cb}|$) and the $B_s^0 \rightarrow D_s^-$ form factor integral, respectively. Combining the systematic uncertainties, the branching fraction is $\mathcal{B}(B_s^0 \rightarrow K^- \mu^+ \nu_\mu) = (1.06 \pm 0.05 \text{ (stat)} \pm 0.08 \text{ (syst)}) \times 10^{-4}$.

The ratio of CKM elements $|V_{ub}|/|V_{cb}|$ is obtained through the relation $R_{\text{BF}} = |V_{ub}|^2/|V_{cb}|^2 \times \text{FF}_K/\text{FF}_{D_s}$. For the FF_K value, a recent LQCD prediction is used for the high q^2 range, $\text{FF}_K(q^2 > 7 \text{ GeV}^2/c^4) = 3.32 \pm 0.46 \text{ ps}^{-1}$ [30], while a LCSR calculation [31] is used for the low q^2 range, $\text{FF}_K(q^2 < 7 \text{ GeV}^2/c^4) = 4.14 \pm 0.38 \text{ ps}^{-1}$, due to the lower accuracy of LQCD calculations in this region. The obtained values are

$$|V_{ub}|/|V_{cb}|(\text{low}) = 0.0607 \pm 0.0015 \text{ (stat)} \pm 0.0013 \text{ (syst)} \pm 0.0008 \text{ } (D_s) \pm 0.0030 \text{ (FF)},$$

$$|V_{ub}|/|V_{cb}|(\text{high}) = 0.0946 \pm 0.0030 \text{ (stat)}^{+0.0024}_{-0.0025} \text{ (syst)} \pm 0.0013 \text{ } (D_s) \pm 0.0068 \text{ (FF)},$$

where the latter two uncertainties are from the D_s^- branching fraction and the form factor integrals. The discrepancy between the values of $|V_{ub}|/|V_{cb}|$ for the low and high q^2 ranges is related to the difference in the theoretical calculations of the form factors. To illustrate this, the LQCD calculation in Ref. [30] gives $\text{FF}_K = 0.94 \pm 0.48 \text{ ps}^{-1}$ at low q^2 , which can be compared to the chosen LCSR value, $4.14 \pm 0.38 \text{ ps}^{-1}$ [31]. Figure 2 depicts the $|V_{ub}|/|V_{cb}|$ measurements of this Letter, $|V_{ub}|/|V_{cb}|(\text{low}) = 0.061 \pm 0.004$ and $|V_{ub}|/|V_{cb}|(\text{high}) = 0.095 \pm 0.008$, with the uncertainties combined. The $|V_{ub}|/|V_{cb}|$ measurement obtained with the Λ_b^0 baryon decays [7], for which a form factor model based on a LQCD calculation [32] was used, is also shown.

In conclusion, the decay $B_s^0 \rightarrow K^- \mu^+ \nu_\mu$ is observed for the first time. The branching fraction ratios in the two q^2 regions reported in this Letter represent the first experimental ingredient to the form factor calculations of the $B_s^0 \rightarrow K^- \mu^+ \nu_\mu$ decay. Moreover, the $|V_{ub}|/|V_{cb}|$ results will improve both the averages of the exclusive measurements in the $(|V_{cb}|, |V_{ub}|)$ plane and the precision on the least known side of the CKM unitarity triangle.

Acknowledgements

We express our gratitude to our colleagues in the CERN accelerator departments for the excellent performance of the LHC. We thank the technical and administrative staff at the LHCb institutes. We acknowledge support from CERN and from the national agencies: CAPES, CNPq, FAPERJ and FINEP (Brazil); MOST and NSFC (China); CNRS/IN2P3 (France); BMBF, DFG and MPG (Germany); INFN (Italy); NWO (Netherlands); MNiSW and NCN (Poland); MEN/IFA (Romania); MSHE (Russia); MICINN (Spain); SNSF and SER (Switzerland); NASU (Ukraine); STFC (United Kingdom); DOE NP and NSF (USA). We acknowledge the computing resources that are provided by CERN, IN2P3 (France), KIT and DESY (Germany), INFN (Italy), SURF (Netherlands), PIC (Spain), GridPP (United Kingdom), RRCKI and Yandex LLC (Russia), CSCS (Switzerland), IFIN-HH (Romania), CBPF (Brazil), PL-GRID (Poland) and OSC (USA). We are indebted to the communities behind the multiple open-source software packages on which we depend. Individual groups or members have received support from AvH Foundation (Germany); EPLANET, Marie Skłodowska-Curie Actions and ERC (European Union); A*MIDEX, ANR, Labex P2IO and OCEVU, and Région Auvergne-Rhône-Alpes (France); Key Research Program of Frontier Sciences of CAS, CAS PIFI, CAS CCEPP, Fundamental Research Funds for Central Universities, and Sci. & Tech. Program of Guangzhou (China); RFBR, RSF and Yandex LLC (Russia); GVA, XuntaGal and GENCAT (Spain); the Royal Society and the Leverhulme Trust (United Kingdom).

References

- [1] N. Cabibbo, *Unitary symmetry and leptonic decays*, Phys. Rev. Lett **10** (1963) 531.
- [2] M. Kobayashi and T. Maskawa, *CP-Violation in the renormalizable theory of weak interaction*, Prog. Theor. Phys **49** (1973) 652.
- [3] N. Isgur, D. Scora, B. Grinstein, and M. B. Wise, *Semileptonic B and D decays in the quark model*, Phys. Rev. **D39** (1989) 799.
- [4] M. J. Dugan and B. Grinstein, *QCD basis for factorization in decays of heavy mesons*, Phys. Lett. **B255** (1991) 583.
- [5] D. Abbaneo *et al.*, *The CKM matrix and the unitarity triangle. Workshop, CERN, Geneva, Switzerland, 13-16 Feb 2002: Proceedings*, CERN Yellow Reports: Conference Proceedings, 2003, arXiv:hep-ph/0304132.
- [6] Heavy Flavor Averaging Group, Y. Amhis *et al.*, *Averages of b-hadron, c-hadron, and τ -lepton properties as of 2018*, arXiv:1909.12524, updated results and plots available at <https://hflav.web.cern.ch>.
- [7] LHCb collaboration, R. Aaij *et al.*, *Determination of the quark coupling strength $|V_{ub}|$ using baryonic decays*, Nature Physics **11** (2015) 743, arXiv:1504.01568.
- [8] CKMfitter Group, J. Charles *et al.*, *CP violation and the CKM matrix: assessing the impact of the asymmetric B factories*, Eur. Phys. J. **C41**

(2005) 1, arXiv:hep-ph/0406184, updated results and plots available at <http://ckmfitter.in2p3.fr>.

- [9] UTfit collaboration, M. Bona *et al.*, *The Unitarity Triangle Fit in the Standard Model and hadronic parameters from lattice QCD: a reappraisal after the measurements of Δm_s and $BR(B \rightarrow \tau\nu)$* , JHEP **10** (2006) 081, arXiv:hep-ph/0606167, updated results and plots available at <http://www.utfit.org/UTfit/>.
- [10] P. Colangelo and A. Khodjamirian, *QCD sum rules, a modern perspective*, At the frontier of particle physics 1495–1576, World Scientific, 2000. arXiv:hep-ph/0010175, report number: CERN-TH-2000-296, BARI-TH-2000-394.
- [11] C. A. Dominguez, *Introduction to QCD sum rules*, Mod. Phys. Lett. **A28** (2013) 1360002, arXiv:1305.7047.
- [12] H. J. Rothe, *Lattice Gauge Theories: An Introduction; 4th ed.*, World Scientific Lecture Notes in Physics, World Scientific, Singapore, 2012.
- [13] LHCb collaboration, A. A. Alves Jr. *et al.*, *The LHCb detector at the LHC*, JINST **3** (2008) S08005.
- [14] LHCb collaboration, R. Aaij *et al.*, *LHCb detector performance*, Int. J. Mod. Phys. **A30** (2015) 1530022, arXiv:1412.6352.
- [15] R. Aaij *et al.*, *The LHCb trigger and its performance in 2011*, JINST **8** (2013) P04022, arXiv:1211.3055.
- [16] T. Sjöstrand, S. Mrenna, and P. Skands, *A brief introduction to PYTHIA 8.1*, Comput. Phys. Commun. **178** (2008) 852, arXiv:0710.3820; T. Sjöstrand, S. Mrenna, and P. Skands, *PYTHIA 6.4 physics and manual*, JHEP **05** (2006) 026, arXiv:hep-ph/0603175.
- [17] D. J. Lange, *The EvtGen particle decay simulation package*, Nucl. Instrum. Meth. **A462** (2001) 152.
- [18] Geant4 collaboration, J. Allison *et al.*, *Geant4 developments and applications*, IEEE Trans. Nucl. Sci. **53** (2006) 270; Geant4 collaboration, S. Agostinelli *et al.*, *Geant4: A simulation toolkit*, Nucl. Instrum. Meth. **A506** (2003) 250.
- [19] V. V. Gligorov and M. Williams, *Efficient, reliable and fast high-level triggering using a bonsai boosted decision tree*, JINST **8** (2013) P02013, arXiv:1210.6861.
- [20] L. Breiman, J. H. Friedman, R. A. Olshen, and C. J. Stone, *Classification and regression trees*, Wadsworth international group, Belmont, California, USA, 1984.
- [21] R. E. Schapire and Y. Freund, *A decision-theoretic generalization of on-line learning and an application to boosting*, Jour. Comp. and Syst. Sc. **55** (1997) 119.
- [22] SLD collaboration, K. Abe *et al.*, *A measurement of $R(b)$ using a vertex mass tag*, Phys. Rev. Lett. **80** (1998) 660, arXiv:hep-ex/9708015.

- [23] G. Ciezarek, A. Lupato, M. Rotondo, and M. Vesterinen, *Reconstruction of semileptonically decaying beauty hadrons produced in high energy pp collisions*, JHEP **02** (2017) 021, [arXiv:1611.08522](#).
- [24] R. J. Barlow and C. Beeston, *Fitting using finite Monte Carlo samples*, Comput. Phys. Commun. **77** (1993) 219.
- [25] Particle Data Group, P. A. Zyla *et al.*, *Review of particle physics*, Prog. Theor. Exp. Phys. **2020** (2020) 083C01.
- [26] LHCb collaboration, L. Anderlini *et al.*, *The PIDCalib package*, LHCb-PUB-2016-021, 2016.
- [27] E. McLean, C. T. H. Davies, J. Koponen, and A. T. Lytle, *$B_s \rightarrow D_s \ell \nu$ Form Factors for the full q^2 range from Lattice QCD with non-perturbatively normalized currents*, Phys. Rev. **D101** (2020) 074513, [arXiv:1906.00701](#).
- [28] C. M. Bouchard *et al.*, *$B_s \rightarrow K \ell \nu$ form factors from lattice QCD*, Phys. Rev. **D90** (2014) 054506, [arXiv:1406.2279](#).
- [29] J. M. Flynn *et al.*, *$B \rightarrow \pi \ell \nu$ and $B_s \rightarrow K \ell \nu$ form factors and $|V_{ub}|$ from 2+1-flavor lattice QCD with domain-wall light quarks and relativistic heavy quarks*, Phys. Rev. **D91** (2015) 074510, [arXiv:1501.05373](#).
- [30] Fermilab Lattice, MILC collaborations, A. Bazavov *et al.*, *$B_s \rightarrow K \ell \nu$ decay from lattice QCD*, Phys. Rev. **D100** (2019) 034501, [arXiv:1901.02561](#).
- [31] A. Khodjamirian and A. V. Rusov, *$B_s \rightarrow K \ell \nu_\ell$ and $B_{(s)} \rightarrow \pi(K) \ell^+ \ell^-$ decays at large recoil and CKM matrix elements*, JHEP **08** (2017) 112, [arXiv:1703.04765](#).
- [32] W. Detmold, C. Lehner, and S. Meinel, *$\Lambda_b^0 \rightarrow p \ell^- \bar{\nu}_\ell$ and $\Lambda_b^0 \rightarrow \Lambda_c^+ \ell^- \bar{\nu}_\ell$ form factors from lattice QCD with relativistic heavy quarks*, Phys. Rev. **D92** (2015) 034503, [arXiv:1503.01421](#).

LHCb collaboration

R. Aaij³², C. Abellán Beteta⁵⁰, T. Ackernley⁶⁰, B. Adeva⁴⁶, M. Adinolfi⁵⁴, H. Afsharnia⁹, C.A. Aidala⁸⁵, S. Aiola²⁶, Z. Ajaltouni⁹, S. Akar⁶⁵, J. Albrecht¹⁵, F. Alessio⁴⁸, M. Alexander⁵⁹, A. Alfonso Albero⁴⁵, Z. Aliouche⁶², G. Alkhazov³⁸, P. Alvarez Cartelle⁴⁸, S. Amato², Y. Amhis¹¹, L. An²², L. Anderlini²², A. Andreianov³⁸, M. Andreotti²¹, F. Archilli¹⁷, A. Artamonov⁴⁴, M. Artuso⁶⁸, K. Arzymatov⁴², E. Aslanides¹⁰, M. Atzeni⁵⁰, B. Audurier¹², S. Bachmann¹⁷, M. Bachmayer⁴⁹, J.J. Back⁵⁶, S. Baker⁶¹, P. Baladron Rodriguez⁴⁶, V. Balagura¹², W. Baldini^{21,48}, J. Baptista Leite¹, R.J. Barlow⁶², S. Barsuk¹¹, W. Barter⁶¹, M. Bartolini^{24,h}, F. Baryshnikov⁸¹, J.M. Basels¹⁴, G. Bassi²⁹, B. Batsukh⁶⁸, A. Battig¹⁵, A. Bay⁴⁹, M. Becker¹⁵, F. Bedeschi²⁹, I. Bediaga¹, A. Beiter⁶⁸, V. Belavin⁴², S. Belin²⁷, V. Bellee⁴⁹, K. Belous⁴⁴, I. Belov⁴⁰, I. Belyaev³⁹, G. Bencivenni²³, E. Ben-Haim¹³, A. Berezhnoy⁴⁰, R. Bernet⁵⁰, D. Berninghoff¹⁷, H.C. Bernstein⁶⁸, C. Bertella⁴⁸, E. Bertholet¹³, A. Bertolin²⁸, C. Betancourt⁵⁰, F. Betti^{20,d}, M.O. Bettler⁵⁵, Ia. Bezshyiko⁵⁰, S. Bhasin⁵⁴, J. Bhom³⁴, L. Bian⁷³, M.S. Bieker¹⁵, S. Bifani⁵³, P. Billoir¹³, M. Birch⁶¹, F.C.R. Bishop⁵⁵, A. Bizzeti^{22,r}, M. Bjørn⁶³, M.P. Blago⁴⁸, T. Blake⁵⁶, F. Blanc⁴⁹, S. Blusk⁶⁸, D. Bobulska⁵⁹, J.A. Boelhauve¹⁵, O. Boente Garcia⁴⁶, T. Boettcher⁶⁴, A. Boldyrev⁸², A. Bondar⁴³, N. Bondar³⁸, S. Borghi⁶², M. Borisjak⁴², M. Borsato¹⁷, J.T. Borsuk³⁴, S.A. Bouchiba⁴⁹, T.J.V. Bowcock⁶⁰, A. Boyer⁴⁸, C. Bozzi²¹, M.J. Bradley⁶¹, S. Braun⁶⁶, A. Brea Rodriguez⁴⁶, M. Brodski⁴⁸, J. Brodzicka³⁴, A. Brossa Gonzalo⁵⁶, D. Brundu²⁷, A. Buonaura⁵⁰, C. Burr⁴⁸, A. Bursche²⁷, A. Butkevich⁴¹, J.S. Butter³², J. Buytaert⁴⁸, W. Byczynski⁴⁸, S. Cadeddu²⁷, H. Cai⁷³, R. Calabrese^{21,f}, L. Calefice^{15,13}, L. Calero Diaz²³, S. Cali²³, R. Calladine⁵³, M. Calvi^{25,i}, M. Calvo Gomez⁸⁴, P. Camargo Magalhaes⁵⁴, A. Camboni⁴⁵, P. Campana²³, D.H. Campora Perez⁴⁸, A.F. Campoverde Quezada⁵, S. Capelli^{25,i}, L. Capriotti^{20,d}, A. Carbone^{20,d}, G. Carboni³⁰, R. Cardinale^{24,h}, A. Cardini²⁷, I. Carli⁶, P. Carniti^{25,i}, L. Carus¹⁴, K. Carvalho Akiba³², A. Casais Vidal⁴⁶, G. Casse⁶⁰, M. Cattaneo⁴⁸, G. Cavallero⁴⁸, S. Celani⁴⁹, J. Cerasoli¹⁰, A.J. Chadwick⁶⁰, M.G. Chapman⁵⁴, M. Charles¹³, Ph. Charpentier⁴⁸, G. Chatzikonstantinidis⁵³, C.A. Chavez Barajas⁶⁰, M. Chefdeville⁸, C. Chen³, S. Chen²⁷, A. Chernov³⁴, S.-G. Chitic⁴⁸, V. Chobanova⁴⁶, S. Cholak⁴⁹, M. Chrzaszcz³⁴, A. Chubykin³⁸, V. Chulikov³⁸, P. Ciambrone²³, M.F. Cicala⁵⁶, X. Cid Vidal⁴⁶, G. Ciezarek⁴⁸, P.E.L. Clarke⁵⁸, M. Clemencic⁴⁸, H.V. Cliff⁵⁵, J. Closier⁴⁸, J.L. Cobbledick⁶², V. Coco⁴⁸, J.A.B. Coelho¹¹, J. Cogan¹⁰, E. Cogneras⁹, L. Cojocariu³⁷, P. Collins⁴⁸, T. Colombo⁴⁸, L. Congedo^{19,c}, A. Contu²⁷, N. Cooke⁵³, G. Coombs⁵⁹, G. Corti⁴⁸, C.M. Costa Sobral⁵⁶, B. Couturier⁴⁸, D.C. Craik⁶⁴, J. Crkovská⁶⁷, M. Cruz Torres¹, R. Currie⁵⁸, C.L. Da Silva⁶⁷, E. Dall'Occo¹⁵, J. Dalseno⁴⁶, C. D'Ambrosio⁴⁸, A. Danilina³⁹, P. d'Argent⁴⁸, A. Davis⁶², O. De Aguiar Francisco⁶², K. De Bruyn⁷⁸, S. De Capua⁶², M. De Cian⁴⁹, J.M. De Miranda¹, L. De Paula², M. De Serio^{19,c}, D. De Simone⁵⁰, P. De Simone²³, J.A. de Vries⁷⁹, C.T. Dean⁶⁷, W. Dean⁸⁵, D. Decamp⁸, L. Del Buono¹³, B. Delaney⁵⁵, H.-P. Dembinski¹⁵, A. Dendek³⁵, V. Denysenko⁵⁰, D. Derkach⁸², O. Deschamps⁹, F. Desse¹¹, F. Dettori^{27,e}, B. Dey⁷³, P. Di Nezza²³, S. Didenko⁸¹, L. Dieste Maronas⁴⁶, H. Dijkstra⁴⁸, V. Dobishuk⁵², A.M. Donohoe¹⁸, F. Dordei²⁷, A.C. dos Reis¹, L. Douglas⁵⁹, A. Dovbnya⁵¹, A.G. Downes⁸, K. Dreimanis⁶⁰, M.W. Dudek³⁴, L. Dufour⁴⁸, V. Duk⁷⁷, P. Durante⁴⁸, J.M. Durham⁶⁷, D. Dutta⁶², M. Dziewiecki¹⁷, A. Dziurda³⁴, A. Dzyuba³⁸, S. Easo⁵⁷, U. Egede⁶⁹, V. Egorychev³⁹, S. Eidelman^{43,u}, S. Eisenhardt⁵⁸, S. Ek-In⁴⁹, L. Eklund⁵⁹, S. Ely⁶⁸, A. Ene³⁷, E. Epple⁶⁷, S. Escher¹⁴, J. Eschle⁵⁰, S. Esen³², T. Evans⁴⁸, A. Falabella²⁰, J. Fan³, Y. Fan⁵, B. Fang⁷³, N. Farley⁵³, S. Farry⁶⁰, D. Fazzini^{25,i}, P. Fedin³⁹, M. Féo⁴⁸, P. Fernandez Declara⁴⁸, A. Fernandez Prieto⁴⁶, J.M. Fernandez-tenllado Arribas⁴⁵, F. Ferrari^{20,d}, L. Ferreira Lopes⁴⁹, F. Ferreira Rodrigues², S. Ferreres Sole³², M. Ferrillo⁵⁰, M. Ferro-Luzzi⁴⁸, S. Filippov⁴¹, R.A. Fini¹⁹, M. Fiorini^{21,f}, M. Firlej³⁵, K.M. Fischer⁶³, C. Fitzpatrick⁶², T. Fiutowski³⁵, F. Fleuret¹², M. Fontana¹³, F. Fontanelli^{24,h}, R. Forty⁴⁸, V. Franco Lima⁶⁰, M. Franco Sevilla⁶⁶,

M. Frank⁴⁸, E. Franzoso²¹, G. Frau¹⁷, C. Frei⁴⁸, D.A. Friday⁵⁹, J. Fu²⁶, Q. Fuehring¹⁵,
 W. Funk⁴⁸, E. Gabriel³², T. Gaintseva⁴², A. Gallas Torreira⁴⁶, D. Galli^{20,d}, S. Gambetta^{58,48},
 Y. Gan³, M. Gandelman², P. Gandini²⁶, Y. Gao⁴, M. Garau²⁷, L.M. Garcia Martin⁵⁶,
 P. Garcia Moreno⁴⁵, J. García Pardiñas⁵⁰, B. Garcia Plana⁴⁶, F.A. Garcia Rosales¹²,
 L. Garrido⁴⁵, C. Gaspar⁴⁸, R.E. Geertsema³², D. Gerick¹⁷, L.L. Gerken¹⁵, E. Gersabeck⁶²,
 M. Gersabeck⁶², T. Gershon⁵⁶, D. Gerstel¹⁰, Ph. Ghez⁸, V. Gibson⁵⁵, M. Giovannetti^{23,j},
 A. Gioventù⁴⁶, P. Gironella Gironell⁴⁵, L. Giubega³⁷, C. Giugliano^{21,48,f}, K. Gizdov⁵⁸,
 E.L. Gkougkousis⁴⁸, V.V. Gligorov¹³, C. Göbel⁷⁰, E. Golobardes⁸⁴, D. Golubkov³⁹,
 A. Golutvin^{61,81}, A. Gomes^{1,a}, S. Gomez Fernandez⁴⁵, F. Goncalves Abrantes⁷⁰, M. Goncerz³⁴,
 G. Gong³, P. Gorbounov³⁹, I.V. Gorelov⁴⁰, C. Gotti^{25,i}, E. Govorkova⁴⁸, J.P. Grabowski¹⁷,
 R. Graciani Diaz⁴⁵, T. Grammatico¹³, L.A. Granado Cardoso⁴⁸, E. Graugés⁴⁵, E. Graverini⁴⁹,
 G. Graziani²², A. Grecu³⁷, L.M. Greeven³², P. Griffith²¹, L. Grillo⁶², S. Gromov⁸¹,
 B.R. Gruberg Cazon⁶³, C. Gu³, M. Guarise²¹, P. A. Günther¹⁷, E. Gushchin⁴¹, A. Guth¹⁴,
 Y. Guz^{44,48}, T. Gys⁴⁸, T. Hadavizadeh⁶⁹, G. Haefeli⁴⁹, C. Haen⁴⁸, J. Haimberger⁴⁸,
 T. Halewood-leagas⁶⁰, P.M. Hamilton⁶⁶, Q. Han⁷, X. Han¹⁷, T.H. Hancock⁶³,
 S. Hansmann-Menzemer¹⁷, N. Harnew⁶³, T. Harrison⁶⁰, C. Hasse⁴⁸, M. Hatch⁴⁸, J. He⁵,
 M. Hecker⁶¹, K. Heijhoff³², K. Heinicke¹⁵, A.M. Hennequin⁴⁸, K. Hennessy⁶⁰, L. Henry^{26,47},
 J. Heuel¹⁴, A. Hicheur², D. Hill⁶³, M. Hilton⁶², S.E. Hollitt¹⁵, J. Hu¹⁷, J. Hu⁷², W. Hu⁷,
 W. Huang⁵, X. Huang⁷³, W. Hulsbergen³², R.J. Hunter⁵⁶, M. Hushchyn⁸², D. Hutchcroft⁶⁰,
 D. Hynds³², P. Ibis¹⁵, M. Idzik³⁵, D. Ilin³⁸, P. Ilten⁶⁵, A. Inglessi³⁸, A. Ishteev⁸¹, K. Ivshin³⁸,
 R. Jacobsson⁴⁸, S. Jakobsen⁴⁸, E. Jans³², B.K. Jashal⁴⁷, A. Jawahery⁶⁶, V. Jevtic¹⁵,
 M. Jezabek³⁴, F. Jiang³, M. John⁶³, D. Johnson⁴⁸, C.R. Jones⁵⁵, T.P. Jones⁵⁶, B. Jost⁴⁸,
 N. Jurik⁴⁸, S. Kandybei⁵¹, Y. Kang³, M. Karacson⁴⁸, M. Karpov⁸², N. Kazeev⁸², F. Keizer^{55,48},
 M. Kenzie⁵⁶, T. Ketel³³, B. Khanji¹⁵, A. Kharisova⁸³, S. Kholodenko⁴⁴, K.E. Kim⁶⁸, T. Kirn¹⁴,
 V.S. Kirsebom⁴⁹, O. Kitouni⁶⁴, S. Klaver³², K. Klimaszewski³⁶, S. Koliiev⁵², A. Kondybayeva⁸¹,
 A. Konoplyannikov³⁹, P. Kopciewicz³⁵, R. Kopecna¹⁷, P. Koppenburg³², M. Korolev⁴⁰,
 I. Kostiuk^{32,52}, O. Kot⁵², S. Kotriakhova^{38,31}, P. Kravchenko³⁸, L. Kravchuk⁴¹,
 R.D. Krawczyk⁴⁸, M. Kreps⁵⁶, F. Kress⁶¹, S. Kretzschmar¹⁴, P. Krokovny^{43,u}, W. Krupa³⁵,
 W. Krzemien³⁶, W. Kucewicz^{34,k}, M. Kucharczyk³⁴, V. Kudryavtsev^{43,u}, H.S. Kuindersma³²,
 G.J. Kunde⁶⁷, T. Kvaratskheliya³⁹, D. Lacarrere⁴⁸, G. Lafferty⁶², A. Lai²⁷, A. Lampis²⁷,
 D. Lancierini⁵⁰, J.J. Lane⁶², R. Lane⁵⁴, G. Lanfranchi²³, C. Langenbruch¹⁴, J. Langer¹⁵,
 O. Lantwin^{50,81}, T. Latham⁵⁶, F. Lazzari^{29,s}, R. Le Gac¹⁰, S.H. Lee⁸⁵, R. Lefèvre⁹, A. Leflat⁴⁰,
 S. Legotin⁸¹, O. Leroy¹⁰, T. Lesiak³⁴, B. Leverington¹⁷, H. Li⁷², L. Li⁶³, P. Li¹⁷, Y. Li⁶, Y. Li⁶,
 Z. Li⁶⁸, X. Liang⁶⁸, T. Lin⁶¹, R. Lindner⁴⁸, V. Lisovskyi¹⁵, R. Litvinov²⁷, G. Liu⁷², H. Liu⁵,
 S. Liu⁶, X. Liu³, A. Loi²⁷, J. Lomba Castro⁴⁶, I. Longstaff⁵⁹, J.H. Lopes², G. Loustau⁵⁰,
 G.H. Lovell⁵⁵, Y. Lu⁶, D. Lucchesi^{28,l}, S. Luchuk⁴¹, M. Lucio Martinez³², V. Lukashenko³²,
 Y. Luo³, A. Lupato⁶², E. Luppi^{21,f}, O. Lupton⁵⁶, A. Lusiani^{29,q}, X. Lyu⁵, L. Ma⁶,
 S. Maccolini^{20,d}, F. Machefert¹¹, F. Maciuc³⁷, V. Macko⁴⁹, P. Mackowiak¹⁵,
 S. Maddrell-Mander⁵⁴, O. Madejczyk³⁵, L.R. Madhan Mohan⁵⁴, O. Maev³⁸, A. Maevskiy⁸²,
 D. Maisuzenko³⁸, M.W. Majewski³⁵, J.J. Malczewski³⁴, S. Malde⁶³, B. Malecki⁴⁸, A. Malinin⁸⁰,
 T. Maltsev^{43,u}, H. Malygina¹⁷, G. Manca^{27,e}, G. Mancinelli¹⁰, R. Manera Escalero⁴⁵,
 D. Manuzzi^{20,d}, D. Marangotto^{26,n}, J. Maratas^{9,t}, J.F. Marchand⁸, U. Marconi²⁰,
 S. Mariani^{22,48,g}, C. Marin Benito¹¹, M. Marinangeli⁴⁹, P. Marino⁴⁹, J. Marks¹⁷,
 P.J. Marshall⁶⁰, G. Martellotti³¹, L. Martinazzoli^{48,i}, M. Martinelli^{25,i}, D. Martinez Santos⁴⁶,
 F. Martinez Vidal⁴⁷, A. Massafferri¹, M. Materok¹⁴, R. Matev⁴⁸, A. Mathad⁵⁰, Z. Mathe⁴⁸,
 V. Matiunin³⁹, C. Matteuzzi²⁵, K.R. Mattioli⁸⁵, A. Mauri³², E. Maurice¹², J. Mauricio⁴⁵,
 M. Mazurek³⁶, M. McCann⁶¹, L. McConnell¹⁸, T.H. McGrath⁶², A. McNab⁶², R. McNulty¹⁸,
 J.V. Mead⁶⁰, B. Meadows⁶⁵, C. Meaux¹⁰, G. Meier¹⁵, N. Meinert⁷⁶, D. Melnychuk³⁶,
 S. Meloni^{25,i}, M. Merk^{32,79}, A. Merli²⁶, L. Meyer Garcia², M. Mikhasenko⁴⁸, D.A. Milanes⁷⁴,
 E. Millard⁵⁶, M. Milovanovic⁴⁸, M.-N. Minard⁸, L. Minzoni^{21,f}, S.E. Mitchell⁵⁸, B. Mitreska⁶²,

D.S. Mitzel⁴⁸, A. Mödden¹⁵, R.A. Mohammed⁶³, R.D. Moise⁶¹, T. Mombächer¹⁵, I.A. Monroy⁷⁴,
 S. Monteil⁹, M. Morandin²⁸, G. Morello²³, M.J. Morello^{29,q}, J. Moron³⁵, A.B. Morris⁷⁵,
 A.G. Morris⁵⁶, R. Mountain⁶⁸, H. Mu³, F. Muheim⁵⁸, M. Mukherjee⁷, M. Mulder⁴⁸,
 D. Müller⁴⁸, K. Müller⁵⁰, C.H. Murphy⁶³, D. Murray⁶², P. Muzzetto^{27,48}, P. Naik⁵⁴,
 T. Nakada⁴⁹, R. Nandakumar⁵⁷, T. Nanut⁴⁹, I. Nasteva², M. Needham⁵⁸, I. Neri^{21,f},
 N. Neri^{26,n}, S. Neubert⁷⁵, N. Neufeld⁴⁸, R. Newcombe⁶¹, T.D. Nguyen⁴⁹, C. Nguyen-Mau⁴⁹,
 E.M. Niel¹¹, S. Nieswand¹⁴, N. Nikitin⁴⁰, N.S. Nolte⁴⁸, C. Nunez⁸⁵, A. Oblakowska-Mucha³⁵,
 V. Obraztsov⁴⁴, D.P. O'Hanlon⁵⁴, R. Oldeman^{27,e}, M.E. Olivares⁶⁸, C.J.G. Onderwater⁷⁸,
 A. Ossowska³⁴, J.M. Otalora Goicochea², T. Ovsianikova³⁹, P. Owen⁵⁰, A. Oyanguren^{47,48},
 B. Pagare⁵⁶, P.R. Pais⁴⁸, T. Pajero^{29,48,q}, A. Palano¹⁹, M. Palutan²³, Y. Pan⁶², G. Panshin⁸³,
 A. Papanestis⁵⁷, M. Pappagallo^{19,c}, L.L. Pappalardo^{21,f}, C. Pappenheimer⁶⁵, W. Parker⁶⁶,
 C. Parkes⁶², C.J. Parkinson⁴⁶, B. Passalacqua²¹, G. Passaleva²², A. Pastore¹⁹, M. Patel⁶¹,
 C. Patrignani^{20,d}, C.J. Pawley⁷⁹, A. Pearce⁴⁸, A. Pellegrino³², M. Pepe Altarelli⁴⁸,
 S. Perazzini²⁰, D. Pereima³⁹, P. Perret⁹, K. Petridis⁵⁴, A. Petrolini^{24,h}, A. Petrov⁸⁰,
 S. Petrucci⁵⁸, M. Petruzzo²⁶, T.T.H. Pham⁶⁸, A. Philippov⁴², L. Pica²⁹, M. Piccini⁷⁷,
 B. Pietrzyk⁸, G. Pietrzyk⁴⁹, M. Pili⁶³, D. Pinci³¹, F. Pisani⁴⁸, A. Piucci¹⁷, Resmi P.K¹⁰,
 V. Placinta³⁷, J. Plews⁵³, M. Plo Casasus⁴⁶, F. Polci¹³, M. Poli Lener²³, M. Poliakova⁶⁸,
 A. Poluektov¹⁰, N. Polukhina^{81,b}, I. Polyakov⁶⁸, E. Polycarpo², G.J. Pomery⁵⁴, S. Ponce⁴⁸,
 D. Popov^{5,48}, S. Popov⁴², S. Poslavskii⁴⁴, K. Prasant³⁴, L. Promberger⁴⁸, C. Prouve⁴⁶,
 V. Pugatch⁵², H. Pullen⁶³, G. Punzi^{29,m}, W. Qian⁵, J. Qin⁵, R. Quagliani¹³, B. Quintana⁸,
 N.V. Raab¹⁸, R.I. Rabadan Trejo¹⁰, B. Rachwal³⁵, J.H. Rademacker⁵⁴, M. Rama²⁹,
 M. Ramos Pernas⁵⁶, M.S. Rangel², F. Ratnikov^{42,82}, G. Raven³³, M. Reboud⁸, F. Redi⁴⁹,
 F. Reiss¹³, C. Remon Alepuz⁴⁷, Z. Ren³, V. Renaudin⁶³, R. Ribatti²⁹, S. Ricciardi⁵⁷,
 K. Rinnert⁶⁰, P. Robbe¹¹, A. Robert¹³, G. Robertson⁵⁸, A.B. Rodrigues⁴⁹, E. Rodrigues⁶⁰,
 J.A. Rodriguez Lopez⁷⁴, A. Rollings⁶³, P. Roloff⁴⁸, V. Romanovskiy⁴⁴, M. Romero Lamas⁴⁶,
 A. Romero Vidal⁴⁶, J.D. Roth⁸⁵, M. Rotondo²³, M.S. Rudolph⁶⁸, T. Ruf⁴⁸, J. Ruiz Vidal⁴⁷,
 A. Ryzhikov⁸², J. Ryzka³⁵, J.J. Saborido Silva⁴⁶, N. Sagidova³⁸, N. Sahoo⁵⁶, B. Saitta^{27,e},
 D. Sanchez Gonzalo⁴⁵, C. Sanchez Gras³², R. Santacesaria³¹, C. Santamarina Rios⁴⁶,
 M. Santimaria²³, E. Santovetti^{30,j}, D. Saranin⁸¹, G. Sarpis⁵⁹, M. Sarpis⁷⁵, A. Sarti³¹,
 C. Satriano^{31,p}, A. Satta³⁰, M. Saur⁵, D. Savrina^{39,40}, H. Sazak⁹, L.G. Scantlebury Smead⁶³,
 S. Schael¹⁴, M. Schellenberg¹⁵, M. Schiller⁵⁹, H. Schindler⁴⁸, M. Schmelling¹⁶, T. Schmelzer¹⁵,
 B. Schmidt⁴⁸, O. Schneider⁴⁹, A. Schopper⁴⁸, M. Schubiger³², S. Schulte⁴⁹, M.H. Schune¹¹,
 R. Schwemmer⁴⁸, B. Sciascia²³, A. Sciubba³¹, S. Sellam⁴⁶, A. Semennikov³⁹,
 M. Senghi Soares³³, A. Sergi^{53,48}, N. Serra⁵⁰, L. Sestini²⁸, A. Seuthe¹⁵, P. Seyfert⁴⁸,
 D.M. Shangase⁸⁵, M. Shapkin⁴⁴, I. Shchemerov⁸¹, L. Shchutska⁴⁹, T. Shears⁶⁰,
 L. Shekhtman^{43,u}, Z. Shen⁴, V. Shevchenko⁸⁰, E.B. Shields^{25,i}, E. Shmanin⁸¹, J.D. Shupperd⁶⁸,
 B.G. Siddi²¹, R. Silva Coutinho⁵⁰, G. Simi²⁸, S. Simone^{19,c}, I. Skiba^{21,f}, N. Skidmore⁷⁵,
 T. Skwarnicki⁶⁸, M.W. Slater⁵³, J.C. Smallwood⁶³, J.G. Smeaton⁵⁵, A. Smetkina³⁹, E. Smith¹⁴,
 I.T. Smith⁵⁸, M. Smith⁶¹, A. Snoch³², M. Soares²⁰, L. Soares Lavra⁹, M.D. Sokoloff⁶⁵,
 F.J.P. Soler⁵⁹, A. Solovev³⁸, I. Solovyev³⁸, F.L. Souza De Almeida², B. Souza De Paula²,
 B. Spaan¹⁵, E. Spadaro Norella^{26,n}, P. Spradlin⁵⁹, F. Stagni⁴⁸, M. Stahl⁶⁵, S. Stahl⁴⁸,
 P. Steffo⁴⁹, O. Steinkamp^{50,81}, S. Stemmlle¹⁷, O. Stenyakin⁴⁴, H. Stevens¹⁵, S. Stone⁶⁸,
 M.E. Stramaglia⁴⁹, M. Stratificiuc³⁷, D. Strekalina⁸¹, S. Strokov⁸³, F. Suljik⁶³, J. Sun²⁷, L. Sun⁷³,
 Y. Sun⁶⁶, P. Svihra⁶², P.N. Swallow⁵³, K. Swientek³⁵, A. Szabelski³⁶, T. Szumlak³⁵,
 M. Szymanski⁴⁸, S. Taneja⁶², F. Teubert⁴⁸, E. Thomas⁴⁸, K.A. Thomson⁶⁰, M.J. Tilley⁶¹,
 V. Tisserand⁹, S. T'Jampens⁸, M. Tobin⁶, S. Tolk⁴⁸, L. Tomassetti^{21,f}, D. Torres Machado¹,
 D.Y. Tou¹³, M. Traill⁵⁹, M.T. Tran⁴⁹, E. Trifonova⁸¹, C. Tripli⁴⁹, G. Tuci^{29,m}, A. Tully⁴⁹,
 N. Tuning³², A. Ukleja³⁶, D.J. Unverzagt¹⁷, E. Ursov⁸¹, A. Usachov³², A. Ustyuzhanin^{42,82},
 U. Uwer¹⁷, A. Vagner⁸³, V. Vagnoni²⁰, A. Valassi⁴⁸, G. Valenti²⁰, N. Valls Canudas⁴⁵,
 M. van Beuzekom³², M. Van Dijk⁴⁹, E. van Herwijnen⁸¹, C.B. Van Hulse¹⁸, M. van Veghel⁷⁸,

R. Vazquez Gomez⁴⁶, P. Vazquez Regueiro⁴⁶, C. Vázquez Sierra³², S. Vecchi²¹, J.J. Velthuis⁵⁴, M. Veltri^{22,o}, A. Venkateswaran⁶⁸, M. Veronesi³², M. Vesterinen⁵⁶, D. Vieira⁶⁵, M. Vieites Diaz⁴⁹, H. Viemann⁷⁶, X. Vilasis-Cardona⁸⁴, E. Vilella Figueras⁶⁰, P. Vincent¹³, G. Vitali²⁹, A. Vollhardt⁵⁰, D. Vom Bruch¹³, A. Vorobyev³⁸, V. Vorobyev^{43,u}, N. Voropaev³⁸, R. Waldi⁷⁶, J. Walsh²⁹, C. Wang¹⁷, J. Wang³, J. Wang⁷³, J. Wang⁴, J. Wang⁶, M. Wang³, R. Wang⁵⁴, Y. Wang⁷, Z. Wang⁵⁰, H.M. Wark⁶⁰, N.K. Watson⁵³, S.G. Weber¹³, D. Websdale⁶¹, C. Weisser⁶⁴, B.D.C. Westhenry⁵⁴, D.J. White⁶², M. Whitehead⁵⁴, D. Wiedner¹⁵, G. Wilkinson⁶³, M. Wilkinson⁶⁸, I. Williams⁵⁵, M. Williams^{64,69}, M.R.J. Williams⁵⁸, F.F. Wilson⁵⁷, W. Wislicki³⁶, M. Witek³⁴, L. Witola¹⁷, G. Wormser¹¹, S.A. Wotton⁵⁵, H. Wu⁶⁸, K. Wyllie⁴⁸, Z. Xiang⁵, D. Xiao⁷, Y. Xie⁷, A. Xu⁴, J. Xu⁵, L. Xu³, M. Xu⁷, Q. Xu⁵, Z. Xu⁵, Z. Xu⁴, D. Yang³, Y. Yang⁵, Z. Yang³, Z. Yang⁶⁶, Y. Yao⁶⁸, L.E. Yeomans⁶⁰, H. Yin⁷, J. Yu⁷¹, X. Yuan⁶⁸, O. Yushchenko⁴⁴, E. Zaffaroni⁴⁹, K.A. Zarebski⁵³, M. Zavertyaev^{16,b}, M. Zdybal³⁴, O. Zenaiev⁴⁸, M. Zeng³, D. Zhang⁷, L. Zhang³, S. Zhang⁴, Y. Zhang⁴, Y. Zhang⁶³, A. Zhelezov¹⁷, Y. Zheng⁵, X. Zhou⁵, Y. Zhou⁵, X. Zhu³, V. Zhukov^{14,40}, J.B. Zonneveld⁵⁸, S. Zucchelli^{20,d}, D. Zuliani²⁸, G. Zunica⁶².

¹*Centro Brasileiro de Pesquisas Físicas (CBPF), Rio de Janeiro, Brazil*

²*Universidade Federal do Rio de Janeiro (UFRJ), Rio de Janeiro, Brazil*

³*Center for High Energy Physics, Tsinghua University, Beijing, China*

⁴*School of Physics State Key Laboratory of Nuclear Physics and Technology, Peking University, Beijing, China*

⁵*University of Chinese Academy of Sciences, Beijing, China*

⁶*Institute Of High Energy Physics (IHEP), Beijing, China*

⁷*Institute of Particle Physics, Central China Normal University, Wuhan, Hubei, China*

⁸*Univ. Grenoble Alpes, Univ. Savoie Mont Blanc, CNRS, IN2P3-LAPP, Annecy, France*

⁹*Université Clermont Auvergne, CNRS/IN2P3, LPC, Clermont-Ferrand, France*

¹⁰*Aix Marseille Univ, CNRS/IN2P3, CPPM, Marseille, France*

¹¹*Université Paris-Saclay, CNRS/IN2P3, IJCLab, Orsay, France*

¹²*Laboratoire Leprince-ringuet (llr), Palaiseau, France*

¹³*LPNHE, Sorbonne Université, Paris Diderot Sorbonne Paris Cité, CNRS/IN2P3, Paris, France*

¹⁴*I. Physikalisches Institut, RWTH Aachen University, Aachen, Germany*

¹⁵*Fakultät Physik, Technische Universität Dortmund, Dortmund, Germany*

¹⁶*Max-Planck-Institut für Kernphysik (MPIK), Heidelberg, Germany*

¹⁷*Physikalischs Institut, Ruprecht-Karls-Universität Heidelberg, Heidelberg, Germany*

¹⁸*School of Physics, University College Dublin, Dublin, Ireland*

¹⁹*INFN Sezione di Bari, Bari, Italy*

²⁰*INFN Sezione di Bologna, Bologna, Italy*

²¹*INFN Sezione di Ferrara, Ferrara, Italy*

²²*INFN Sezione di Firenze, Firenze, Italy*

²³*INFN Laboratori Nazionali di Frascati, Frascati, Italy*

²⁴*INFN Sezione di Genova, Genova, Italy*

²⁵*INFN Sezione di Milano-Bicocca, Milano, Italy*

²⁶*INFN Sezione di Milano, Milano, Italy*

²⁷*INFN Sezione di Cagliari, Monserrato, Italy*

²⁸*Universita degli Studi di Padova, Universita e INFN, Padova, Padova, Italy*

²⁹*INFN Sezione di Pisa, Pisa, Italy*

³⁰*INFN Sezione di Roma Tor Vergata, Roma, Italy*

³¹*INFN Sezione di Roma La Sapienza, Roma, Italy*

³²*Nikhef National Institute for Subatomic Physics, Amsterdam, Netherlands*

³³*Nikhef National Institute for Subatomic Physics and VU University Amsterdam, Amsterdam, Netherlands*

³⁴*Henryk Niewodniczanski Institute of Nuclear Physics Polish Academy of Sciences, Kraków, Poland*

³⁵*AGH - University of Science and Technology, Faculty of Physics and Applied Computer Science, Kraków, Poland*

³⁶*National Center for Nuclear Research (NCBJ), Warsaw, Poland*

- ³⁷*Horia Hulubei National Institute of Physics and Nuclear Engineering, Bucharest-Magurele, Romania*
- ³⁸*Petersburg Nuclear Physics Institute NRC Kurchatov Institute (PNPI NRC KI), Gatchina, Russia*
- ³⁹*Institute of Theoretical and Experimental Physics NRC Kurchatov Institute (ITEP NRC KI), Moscow, Russia*
- ⁴⁰*Institute of Nuclear Physics, Moscow State University (SINP MSU), Moscow, Russia*
- ⁴¹*Institute for Nuclear Research of the Russian Academy of Sciences (INR RAS), Moscow, Russia*
- ⁴²*Yandex School of Data Analysis, Moscow, Russia*
- ⁴³*Budker Institute of Nuclear Physics (SB RAS), Novosibirsk, Russia*
- ⁴⁴*Institute for High Energy Physics NRC Kurchatov Institute (IHEP NRC KI), Protvino, Russia, Protvino, Russia*
- ⁴⁵*ICCUB, Universitat de Barcelona, Barcelona, Spain*
- ⁴⁶*Instituto Galego de Física de Altas Enerxías (IGFAE), Universidade de Santiago de Compostela, Santiago de Compostela, Spain*
- ⁴⁷*Instituto de Fisica Corpuscular, Centro Mixto Universidad de Valencia - CSIC, Valencia, Spain*
- ⁴⁸*European Organization for Nuclear Research (CERN), Geneva, Switzerland*
- ⁴⁹*Institute of Physics, Ecole Polytechnique Fédérale de Lausanne (EPFL), Lausanne, Switzerland*
- ⁵⁰*Physik-Institut, Universität Zürich, Zürich, Switzerland*
- ⁵¹*NSC Kharkiv Institute of Physics and Technology (NSC KIPT), Kharkiv, Ukraine*
- ⁵²*Institute for Nuclear Research of the National Academy of Sciences (KINR), Kyiv, Ukraine*
- ⁵³*University of Birmingham, Birmingham, United Kingdom*
- ⁵⁴*H.H. Wills Physics Laboratory, University of Bristol, Bristol, United Kingdom*
- ⁵⁵*Cavendish Laboratory, University of Cambridge, Cambridge, United Kingdom*
- ⁵⁶*Department of Physics, University of Warwick, Coventry, United Kingdom*
- ⁵⁷*STFC Rutherford Appleton Laboratory, Didcot, United Kingdom*
- ⁵⁸*School of Physics and Astronomy, University of Edinburgh, Edinburgh, United Kingdom*
- ⁵⁹*School of Physics and Astronomy, University of Glasgow, Glasgow, United Kingdom*
- ⁶⁰*Oliver Lodge Laboratory, University of Liverpool, Liverpool, United Kingdom*
- ⁶¹*Imperial College London, London, United Kingdom*
- ⁶²*Department of Physics and Astronomy, University of Manchester, Manchester, United Kingdom*
- ⁶³*Department of Physics, University of Oxford, Oxford, United Kingdom*
- ⁶⁴*Massachusetts Institute of Technology, Cambridge, MA, United States*
- ⁶⁵*University of Cincinnati, Cincinnati, OH, United States*
- ⁶⁶*University of Maryland, College Park, MD, United States*
- ⁶⁷*Los Alamos National Laboratory (LANL), Los Alamos, United States*
- ⁶⁸*Syracuse University, Syracuse, NY, United States*
- ⁶⁹*School of Physics and Astronomy, Monash University, Melbourne, Australia, associated to ⁵⁶*
- ⁷⁰*Pontifícia Universidade Católica do Rio de Janeiro (PUC-Rio), Rio de Janeiro, Brazil, associated to ²*
- ⁷¹*Physics and Micro Electronic College, Hunan University, Changsha City, China, associated to ⁷*
- ⁷²*Guangdong Provincial Key Laboratory of Nuclear Science, Institute of Quantum Matter, South China Normal University, Guangzhou, China, associated to ³*
- ⁷³*School of Physics and Technology, Wuhan University, Wuhan, China, associated to ³*
- ⁷⁴*Departamento de Física, Universidad Nacional de Colombia, Bogota, Colombia, associated to ¹³*
- ⁷⁵*Universität Bonn - Helmholtz-Institut für Strahlen und Kernphysik, Bonn, Germany, associated to ¹⁷*
- ⁷⁶*Institut für Physik, Universität Rostock, Rostock, Germany, associated to ¹⁷*
- ⁷⁷*INFN Sezione di Perugia, Perugia, Italy, associated to ²¹*
- ⁷⁸*Van Swinderen Institute, University of Groningen, Groningen, Netherlands, associated to ³²*
- ⁷⁹*Universiteit Maastricht, Maastricht, Netherlands, associated to ³²*
- ⁸⁰*National Research Centre Kurchatov Institute, Moscow, Russia, associated to ³⁹*
- ⁸¹*National University of Science and Technology “MISIS”, Moscow, Russia, associated to ³⁹*
- ⁸²*National Research University Higher School of Economics, Moscow, Russia, associated to ⁴²*
- ⁸³*National Research Tomsk Polytechnic University, Tomsk, Russia, associated to ³⁹*
- ⁸⁴*DS4DS, La Salle, Universitat Ramon Llull, Barcelona, Spain, associated to ⁴⁵*
- ⁸⁵*University of Michigan, Ann Arbor, United States, associated to ⁶⁸*

^a*Universidade Federal do Triângulo Mineiro (UFTM), Uberaba-MG, Brazil*

^b*P.N. Lebedev Physical Institute, Russian Academy of Science (LPI RAS), Moscow, Russia*

^c*Università di Bari, Bari, Italy*

^d Università di Bologna, Bologna, Italy

^e Università di Cagliari, Cagliari, Italy

^f Università di Ferrara, Ferrara, Italy

^g Università di Firenze, Firenze, Italy

^h Università di Genova, Genova, Italy

ⁱ Università di Milano Bicocca, Milano, Italy

^j Università di Roma Tor Vergata, Roma, Italy

^k AGH - University of Science and Technology, Faculty of Computer Science, Electronics and Telecommunications, Kraków, Poland

^l Università di Padova, Padova, Italy

^m Università di Pisa, Pisa, Italy

ⁿ Università degli Studi di Milano, Milano, Italy

^o Università di Urbino, Urbino, Italy

^p Università della Basilicata, Potenza, Italy

^q Scuola Normale Superiore, Pisa, Italy

^r Università di Modena e Reggio Emilia, Modena, Italy

^s Università di Siena, Siena, Italy

^t MSU - Iligan Institute of Technology (MSU-IIT), Iligan, Philippines

^u Novosibirsk State University, Novosibirsk, Russia